INFLUENCE OF POST-BUCKLING BEHAVIOUR ON OPTIMUM DESIGN OF STIFFENED PANELS

Viggo Tvergaard

Department of Solid Mechanics, The Technical University of Denmark, Lyngby, Denmark

Abstract—For an eccentrically stiffened wide panel under compression the optimality of a design with simultaneous occurrence of buckling as a wide Euler column and local buckling of the plate between the stiffeners is investigated. The total amount of material per unit width of the panel is prescribed. As a function of the distribution of this material in the plate and the stiffeners the maximum carrying capacities are calculated approximately by application of Galerkin's method. The design with the highest carrying capacity and the design with the best ability to retain axial stiffness, corresponding to given imperfections, are determined. It is shown that imperfections move the optimum away from the coincident buckling mode design.

INTRODUCTION

FOR compression members built up of thin plates, a design in which column buckling of the whole structure and local buckling of the plate elements occur simultaneously has often been accepted as the optimum design. However, this design criterion is questionable, as was first pointed out by Koiter [1] on the basis that local buckling may promote column failure.

In an investigation of the interaction between local buckling and column failure for a simplified model of a thin-walled column van der Neut [2] has shown that this structure is strongly imperfection-sensitive in the case of coincident buckling loads. Koiter and Kuiken [3] have treated the same problem by application of the general nonlinear theory of elastic stability, and Thompson and Lewis [4] have calculated optimal designs of idealized columns with equally imperfect flanges and no column imperfections. Using Koiter's general theory of elastic stability, the author [5] has shown that a wide integrally stiffened panel under compression is particularly imperfection-sensitive when buckling of the panel as a wide Euler column and local buckling of the plate between the stiffeners occur at the same critical stress.

In the present paper the question of optimality of integrally stiffened panels with coincident buckling loads is further investigated. It is shown in [5] that such two-mode designs are dangerous due to a high sensitivity to small imperfections, but here we shall directly compare the maximum carrying capacities of imperfect panels with different distributions of the available material on the plate and the stiffeners. As we mainly wish to study the connexion between optimum design and coincident buckling load design, the results presented here are restricted to cases with predetermined shapes and positions of the stiffeners. The maximum carrying capacities and the stiffness are calculated approximately by a Galerkin solution of the nonlinear equations of equilibrium.

1. NONLINEAR DIFFERENTIAL EQUATIONS

The panel in consideration is infinitely wide in the y-direction, with a constant spacing b between the stiffeners and the distance a between the simply supported edges on which the compressive load acts (Fig. 1). The plate thickness is h, and the eccentricity e of the stiffeners is taken as positive in the z-direction.
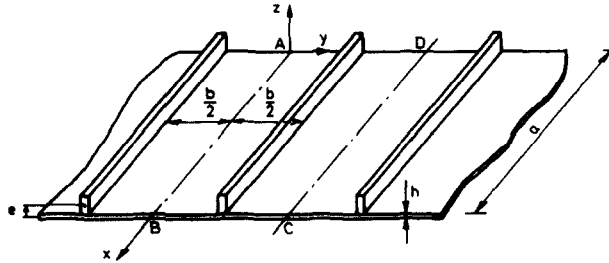
FIG. 1. Part of the wide, stiffened panel.

When u, v and w are the displacements of the middle surface in the x, y and z directions, respectively, and the unloaded, stress-free panel is assumed to have an initial imperfection in the form of a normal displacement $\bar{w}$, the membrane strains of the plate are taken to be

$$
\begin{aligned}
\varepsilon_x &= u_{,x} + \tfrac{1}{2}w^2_{,x} + \bar{w}_{,x}w_{,x} \\
\varepsilon_y &= v_{,y} + \tfrac{1}{2}w^2_{,y} + \bar{w}_{,y}w_{,y} \\
\varepsilon_{xy} &= \tfrac{1}{2}(u_{,y} + v_{,x}) + \tfrac{1}{2}w_{,x}w_{,y} + \tfrac{1}{2}(\bar{w}_{,x}w_{,y} + \bar{w}_{,y}w_{,x})
\end{aligned}
\tag{1.1}
$$

and the bending strains are given by

$$
\kappa_x = w_{,xx}, \qquad \kappa_y = w_{,yy}, \qquad \kappa_{xy} = w_{,xy}.
\tag{1.2}
$$

The bending strain in a stiffener is taken to be the same as in the plate, $w_{,xx}$, and the axial strain of the neutral axis is taken to be

$$
\varepsilon_s = \varepsilon_x - ew_{,xx}.
\tag{1.3}
$$

In [5] the contributions to ε_s from the rotation of the stiffener around its line of attachment to the plate are also included, but the results show that this effect can be neglected for the large range of practical structures with small values of e/b.

The usual stress–strain relationships are assumed for the plate

$$
N_x = \frac{Eh}{1-v^2}(\varepsilon_x + v\varepsilon_y), \qquad M_x = D(\kappa_x + v\kappa_y)
$$

$$
N_{xy} = \frac{Eh}{1+v}\varepsilon_{xy}, \qquad M_{xy} = D(1-v)\kappa_{xy}
\tag{1.4}
$$

$$
N_y = \frac{Eh}{1-v^2}(\varepsilon_y + v\varepsilon_x), \qquad M_y = D(\kappa_y + v\kappa_x)
$$

and for a stiffener

$$
N_s = E_s A_s \varepsilon_s, \qquad M_s = E_s I_s w_{,xx}, \qquad M_{Vs} = G_s K_s w_{,xy}.
\tag{1.5}
$$

Here E, D and G denote Young's modulus, the plate bending stiffness and the shear modulus, respectively, and subscript s refers to a stiffener. The tangential bending stiffness of the stringers is neglected.

Now using the calculus of variations in the virtual work expression and expressing the resultant membrane stresses by means of an Airy stress function

$$N_x = F_{,yy}, \qquad N_{xy} = -F_{,xy}, \qquad N_y = F_{,xx}. \tag{1.6}$$

we find the von Kármán plate equations

$$D \, \Delta\Delta w = F_{,yy}(w_{,xx}+\bar{w}_{,xx}) - 2F_{,xy}(w_{,xy}+\bar{w}_{,xy}) + F_{,xx}(w_{,yy}+\bar{w}_{,yy}) \tag{1.7}$$

$$\frac{1}{Eh} \Delta\Delta F = w_{,xy}^2 - w_{,xx}w_{,yy} + 2\bar{w}_{,xy}w_{,xy} - \bar{w}_{,xx}w_{,yy} - w_{,xx}\bar{w}_{,yy} \tag{1.8}$$

where Δ is the Laplacian operator, and we also find the discontinuity conditions at a stiffener

$$F_{,xy}^+ - F_{,xy}^- - N_{s'x} = 0 \tag{1.9}$$

$$F_{,xx}^- - F_{,xx}^+ = 0 \tag{1.10}$$

$$D(w_{,yyy}^+ - w_{,yyy}^-) + E_s I_s w_{,xxxx}^- - e N_{s'xx} - N_s(w_{,xx}^- + \bar{w}_{,xx}^-) = 0 \tag{1.11}$$

$$D(w_{,yy}^- - w_{,yy}^+) - G_s K_s w_{,xxy}^- = 0 \tag{1.12}$$

$$F_{,yy}^+ - F_{,yy}^- = 0 \tag{1.13}$$

$$(2+v)(F_{,xxy}^+ - F_{,xxy}^-) + (F_{,yyy}^+ - F_{,yyy}^-) = 0 \tag{1.14}$$

$$w^+ - w^- = 0 \tag{1.15}$$

$$w_{,y}^+ - w_{,y}^- = 0 \tag{1.16}$$

where

$$N_s = E_s A_s \left[\frac{1}{Eh}(F_{,yy}^- - vF_{,xx}^-) - e w_{,xx}^- \right]. \tag{1.17}$$

Here superscript $^+$ refers to the side of the stiffener in the positive y-direction and superscript $^-$ refers to the other side.

Periodicity with a period of width p in the y-direction is enforced by the additional condition

$$\int_0^p \left[\frac{1}{Eh}(F_{,xx} - vF_{,yy}) - \tfrac{1}{2}w_{,y}^2 - \bar{w}_{,y}w_{,y} \right] \mathrm{d}y = \text{const.} \tag{1.18}$$

Any equilibrium state of the compressed panel can be written in the form

$$w = w(x, y) \tag{1.19}$$

$$F = \lambda N_x^o \frac{y^2}{2} + f(x, y). \tag{1.20}$$

Here the term $\lambda N_x^o y^2/2$ constitutes the prebuckling solution for the perfect panel ($\bar{w} \equiv 0$), where the stress state is taken to be proportional to a stress state consisting of a constant resultant axial membrane stress N_x^o in the plate and a constant force N_s^o in the stiffeners,

while the transverse deflections vanish identically. The boundary conditions are taken to be

$$w = w_{,xx} = f = f_{,xx} = 0 \tag{1.21}$$

at the simply supported edges for $x = 0, a$.

2. CLASSICAL BUCKLING

For the perfect panel ($\bar{w} \equiv 0$) the classical buckling equations are obtained by substituting the expressions (1.19) and (1.20) in equations (1.7)–(1.16) and then linearizing the resultant equations with respect to w and f. As shown in [5], the critical deflection function w_c and the associated stress function f_c in a plate section between two stiffeners at $y = b/2$ and $y = -b/2$ take the form

$$w_c = (c_1 \cosh(r_1 y) + c_2 \cos(r_2 y)) \sin \frac{k\pi x}{a} \tag{2.1}$$

$$f_c = \left(c_3 \cosh \frac{k\pi y}{a} + c_4 y \sinh \frac{k\pi y}{a}\right) \sin \frac{k\pi x}{a} \tag{2.2}$$

where k is a positive integer, and

$$r_1 = \sqrt{\left\{\frac{k\pi}{a}\left[\frac{k\pi}{a} + \sqrt{\left(-\lambda_c \frac{N_x^o}{D}\right)}\right]\right\}}, \qquad r_2 = \sqrt{\left\{-\frac{k\pi}{a}\left[\frac{k\pi}{a} - \sqrt{\left(-\lambda_c \frac{N_x^o}{D}\right)}\right]\right\}}. \tag{2.3}$$

In the local coordinate system of the next plate section the same expressions apply, but with other constants c_5, c_6, c_7 and c_8 instead of c_1, c_2, c_3 and c_4. Substituting these expressions for w_c and f_c in the linearized discontinuity conditions, we obtain eight linear, homogeneous equations for the constants $c_1, c_2, \ldots, c_8$. The critical buckling load λ_c is the smallest value of the parameter λ, for any integer value of k, for which the determinant of the coefficient matrix vanishes.

As long as the stiffeners are relatively weak, the panel buckles as a wide Euler column, with $k = 1$ and identical modes for all plate sections between two stiffeners. Thus, the constants c_1, c_2, c_3 and c_4 are identical to c_5, c_6, c_7 and c_8, respectively, for this mode. However, when the bending stiffness of the stringers is sufficiently high, local buckling of the plate between the stiffeners is critical, with an integer value of k close to the value of a/b. Except for cases where the torsional stiffness of the stringers is more dominant than their bending stiffness, the critical local mode is one in which the stress function f_c disappears identically, and the constants c_1 and c_2 are identical to $-c_5$ and $-c_6$, respectively.

In the following the Euler-type buckling mode, periodic in the y-direction with one period equal to the spacing between the stiffeners, is denoted $w_c^{(1)}$, $f_c^{(1)}$, and the critical local buckling mode, with one period equal to twice the spacing between the stiffeners, is denoted $w_c^{(2)}$, $f_c^{(2)}$. The buckling modes are orthogonal to one another in the sense

$$\int_0^a \int_0^b N_x^o w_{c,x}^{(i)} w_{c,x}^{(j)} \, dy \, dx + \int_0^a N_s^o [w_{c,x}^{(i)} w_{c,x}^{(j)}]_{y=b/2} \, dx = 0 \tag{2.4}$$

for $i \neq j$.

3. SOLUTION BY THE GALERKIN METHOD

By application of Koiter's general theory of elastic stability [6, 7], the initial post-buckling behaviour of the panel under consideration has been determined in [5]. Here it is found that the structure is particularly imperfection-sensitive in cases when Euler-type buckling and local buckling occur at the same critical stress. In the present work we wish to compare the behaviour of different designs built of a given amount of material per unit width. However, for this purpose the asymptotic results of [5] are not applicable, as their adequacy is limited to very small deflections in cases in which the local buckling stress is slightly above the Euler buckling stress or vice versa. Therefore, the analysis here will be based on an approximate solution of the nonlinear differential equations by application of the Galerkin method. The same approach has been used by Hutchinson [8] to analyse the imperfection-sensitivity of a cylindrical shell under axial compression in cases in which the smallest critical stresses differ slightly from one another due to a superposed internal pressure.

For a given design the Euler-type buckling mode $w_c^{(1)}, f_c^{(1)}$ and the local buckling mode corresponding to the smallest buckling stress $w_c^{(2)}, f_c^{(2)}$ are normalized so that the maximum normal deflection $(w_c)_{max}$ is equal to the maximum possible plate thickness h_o, where

$$h_o = h + A_s/b. \qquad (3.1)$$

As our primary interest is interaction of the Euler-type buckling mode and the local buckling mode, we shall study the behaviour of a panel with small initial imperfections in the form

$$\bar{w} = \bar{\xi}_1 w_c^{(1)} + \bar{\xi}_2 w_c^{(2)} \qquad (3.2)$$

where $\bar{\xi}_1$ and $\bar{\xi}_2$ denote the ratios between the imperfection amplitudes and h_o. For a panel with such imperfections it seems reasonable to approximate w by the expression

$$w = \xi_1 w_c^{(1)} + \xi_2 w_c^{(2)} + \xi_3 w_c^{(3)} + \xi_4 w_c^{(4)} \qquad (3.3)$$

where the parameters ξ_i denote the amounts introduced of the corresponding buckling modes, and $w_c^{(3)}$ is the mode in the form (2.1), with $k = 1$ and the second lowest eigenvalue corresponding to identical deflection functions for all plate sections between two stiffeners. This mode is chosen because it is known from the asymptotic analysis in [5] that when Euler-type buckling takes place, a major part of the second order contribution to the deflections is contained in $w_c^{(3)}$, and when local buckling takes place, the most important part of the second order deflection is accounted for by $w_c^{(1)}$ and $w_c^{(3)}$. The last mode $w_c^{(4)}$ is the lowest local buckling mode in the form (2.1), with one period equal to $2b$ in the y-direction, but with two more half sine waves in the x-direction than corresponding to $w_c^{(2)}$.

As equation (1.8) is a compatibility equation, we prefer to solve it exactly for the stress function f in terms of the assumed deflection function w. Then we are sure that the energy computed from the approximate solution will always be larger than the minimum value corresponding to the true solution of the nonlinear differential equations.

Substituting the assumed deflection function (3.3) in the compatibility equation (1.8) and in the discontinuity conditions (1.9), (1.10), (1.13) and (1.14) that account for tangential equilibrium and tangential compatibility at the stiffeners, we find that the stress function

f can be written in the form

$$f = (\xi_1^2 + 2\xi_1\bar{\xi}_1)f_1 + (\xi_2^2 + 2\xi_2\bar{\xi}_2)f_2 + (\xi_1\xi_2 + \bar{\xi}_1\xi_2 + \xi_1\bar{\xi}_2)f_3$$

$$+ \xi_1 f_4 + \xi_3^2 f_5 + (\xi_3\xi_1 + \xi_3\bar{\xi}_1)f_6 + (\xi_3\xi_2 + \xi_3\bar{\xi}_2)f_7 + \xi_3 f_8$$

$$+ \xi_4^2 f_9 + (\xi_4\xi_1 + \xi_4\bar{\xi}_1)f_{10} + (\xi_4\xi_2 + \xi_4\bar{\xi}_2)f_{11} + \xi_4\xi_3 f_{12} \qquad (3.4)$$

where the twelve functions $f_1, f_2, \ldots, f_{12}$, independent of the amplitude parameters ξ_1, $\xi_2, \xi_3, \xi_4, \bar{\xi}_1$ and $\bar{\xi}_2$, are the solutions of twelve linear boundary value problems. The function f_4 is identical to $f_c^{(1)}$, and the function f_8 is identical to $f_c^{(3)}$. The remaining ten boundary value problems are solved numerically by taking the functions $f_i(x, y)$ as sine-series in the x-direction and using a finite difference method to determine the y-dependent coefficient functions of the series. A sufficient number of terms is included in each series to ensure convergence of the coefficients of the algebraic Galerkin equations.

Knowing the stress function (3.4) corresponding to any mode assumption in the form (3.3), we use the Galerkin method to obtain an approximate solution of the equilibrium equation (1.7) with the discontinuity conditions (1.11), (1.12), (1.15) and (1.16) at the stiffeners. Thus, we choose the parameters ξ_1, ξ_2, ξ_3 and ξ_4 so that the principle of virtual work is satisfied for virtual deflections equal to $w_c^{(1)}, w_c^{(2)}, w_c^{(3)}$ and $w_c^{(4)}$. As the solutions are periodic in the y-direction, we need only carry out integrations over a section ABCD of the panel (Fig. 1), and the conditions to be satisfied are:

$$\int_0^a \int_0^b w_c^{(j)}[D\,\Delta\Delta w - (\lambda N_x^o + f,_{yy})(w,_{xx} + \bar{w},_{xx}) + 2f,_{xy}(w,_{xy} + \bar{w},_{xy})$$

$$- f,_{xx}(w,_{yy} + \bar{w},_{yy})]\,dy\,dx + \int_0^a w_c^{(j)}\left[D(w,_{yyy}^+ - w,_{yyy}^-)\right.$$

$$+ (E_s I_s + e^2 E_s A_s)w,_{xxxx}^- - e\frac{E_s A_s}{Eh}(f,_{yyxx}^- - vf,_{xxxx}^-)$$

$$\left. - \frac{E_s A_s}{Eh}(\lambda N_x^o + f,_{yy}^- - vf,_{xx}^- - eEhw,_{xx}^-)(w,_{xx}^- + \bar{w},_{xx}^-)\right]dx$$

$$+ \int_0^a w_{c,y}^{(j)}[D(w,_{yy}^- - w,_{yy}^+) - G_s K_s w,_{xxy}^-]\,dx = 0 \quad \text{for } j = 1, 2, 3, 4. \qquad (3.5)$$

Here the two last integrals are taken along the stiffener.

Substituting the expressions (3.3) and (3.4) for w and f in equations (3.5) and using the orthogonality condition (2.4) together with the linear eigenvalue problem for classical buckling, we obtain the following nonlinear algebraic equilibrium relations between λ,

ξ_1, ξ_2, ξ_3 and ξ_4

$$
\begin{aligned}
\xi_j(1 - \lambda/\lambda_c^{(j)}) &- \bar{\xi}_j \lambda/\lambda_c^{(j)} + (\xi_1^2 + 2\xi_1\bar{\xi}_1)b_{j1} + (\xi_2^2 + 2\xi_2\bar{\xi}_2)b_{j2} \\
&+ \xi_3^2 b_{j5} + (\xi_3\xi_1 + \xi_3\bar{\xi}_1)b_{j6} + \xi_4^2 b_{j9} + (\xi_4\xi_2 + \xi_4\bar{\xi}_2)b_{j11} \\
&+ (\xi_1^2 + \xi_1\bar{\xi}_1)c_{j11} + (2\xi_1\xi_3 + \bar{\xi}_1\xi_3)c_{j31} + \xi_3^2 c_{j33} \\
&+ \sum_{i=1}^{4} [(\xi_i + \bar{\xi}_i)\{(\xi_1^2 + 2\xi_1\bar{\xi}_1)a_{j1i} + (\xi_2^2 + 2\xi_2\bar{\xi}_2)a_{j2i} \\
&+ (\xi_1\xi_2 + \bar{\xi}_1\xi_2 + \xi_1\bar{\xi}_2)a_{j3i} + \xi_1 a_{j4i} + \xi_3^2 a_{j5i} + (\xi_3\xi_1 + \xi_3\bar{\xi}_1)a_{j6i} \\
&+ (\xi_3\xi_2 + \xi_3\bar{\xi}_2)a_{j7i} + \xi_3 a_{j8i} + \xi_4^2 a_{j9i} + (\xi_4\xi_1 + \xi_4\bar{\xi}_1)a_{j10i} \\
&+ (\xi_4\xi_2 + \xi_4\bar{\xi}_2)a_{j11i} + \xi_4\xi_3 a_{j12i}\}] = 0, \quad \text{for } j = 1, 2, 3, 4
\end{aligned}
\tag{3.6}
$$

where the nondimensional coefficients are given by the expressions

$$
n_i = 2\lambda_c^{(i)} N_x^o \int_0^a \int_0^{b/2} w_c^{(i)} w_{c'xx}^{(i)} \, dy \, dx + \lambda_c^{(i)} N_s^o \int_0^a [w_c^{(i)} w_{c'xx}^{(i)}]_{y=b/2} \, dx
\tag{3.7}
$$

$$
\begin{aligned}
a_{ijk} = \frac{1}{n_i} \Bigg\{ &2 \int_0^a \int_0^{b/2} w_c^{(i)}(-f_{j'yy} w_{c'xx}^{(k)} + 2f_{j'xy} w_{c'xy}^{(k)} - f_{j'xx} w_{c'yy}^{(k)}) \, dy \, dx \\
&- \frac{E_s A_s}{Eh} \int_0^a [w_c^{(i)}(f_{j'yy} - \nu f_{j'xx})w_{c'xx}^{(k)}]_{y=b/2} \, dx \Bigg\}
\end{aligned}
\tag{3.8}
$$

$$
b_{ij} = \frac{1}{n_i} \int_0^a e \frac{E_s A_s}{Eh} [w_c^{(i)}(-f_{j'yyxx} + \nu f_{j'xxxx})]_{y=b/2} \, dx
\tag{3.9}
$$

$$
c_{ijk} = \frac{1}{n_i} \int_0^a e E_s A_s [w_c^{(i)} w_{c'xx}^{(j)} w_{c'xx}^{(k)}]_{y=b/2} \, dx.
\tag{3.10}
$$

In equations (3.6) the constants b_{ji} and c_{jik} vanish for $j = 2, 4$ since the functions $w_c^{(2)}$ and $w_c^{(4)}$ vanish at the stiffeners, and half of the constants a_{jik} vanish because of the periodicity of the functions $w_c^{(i)}$ and f_i with different periods in the y-direction. Furthermore, according to the assumption (3.2), $\bar{\xi}_3$ and $\bar{\xi}_4$ are taken equal to zero.

If the Galerkin method is applied with only the two first terms on the right-hand side of equation (3.3), the algebraic buckling equations reduce to equations (3.6) for $j = 1, 2$ with ξ_3 and ξ_4 equal to zero. Then, in the special case $\lambda_c^{(1)} = \lambda_c^{(2)}$, these two buckling equations coincide with the initial post-buckling equations derived in [5], if terms of order ξ^3, $\xi^2\bar{\xi}$, $\xi\bar{\xi}^2$ and $\xi\bar{\xi}$ are neglected as they were in the asymptotic analysis. However, in the present calculations, we shall retain the higher order terms, as the carrying capacity above the critical buckling stress in part of the range, where local buckling is critical, is described by terms of order ξ^3.

The inclusion of the functions $w_c^{(3)}$ and $w_c^{(4)}$ in the deflection assumption (3.3) results in an appreciable lowering of the maximum carrying capacity for some designs. As a test of the choice of these extra functions, we have tried replacing $w_c^{(3)}$ and $w_c^{(4)}$ by a number of other modes with the same periods b and $2b$, respectively, in the y-direction, which can be done without changing the form of the four Galerkin equations (3.6). However, the reduction in the maximum carrying capacity due to these alternative extra functions was never more than a fraction of the reduction due to $w_c^{(3)}$ and $w_c^{(4)}$, respectively. Therefore,

it is expected that the mode assumption (3.3) leads to a good approximation of the exact solution of the nonlinear differential equations.

4. BEHAVIOUR OF IMPERFECT PANEL

For a panel with known imperfections, the behaviour as the axial compression is increased can be determined from a solution of the nonlinear, algebraic buckling equations.

The four buckling equations (3.6) are written formally as

$$g_i(\lambda, \xi_1, \xi_2, \xi_3, \xi_4) = 0, \quad \text{for } i = 1, 2, 3, 4. \tag{4.1}$$

When, for a given value of ξ_1, we know an approximate solution $\tilde{\lambda}, \tilde{\xi}_2, \tilde{\xi}_3, \tilde{\xi}_4$, the deviations $d\lambda, d\xi_2, d\xi_3, d\xi_4$ from the exact solution satisfy the equations

$$g_i(\tilde{\lambda}+d\lambda, \xi_1, \tilde{\xi}_2+d\xi_2, \tilde{\xi}_3+d\xi_3, \tilde{\xi}_4+d\xi_4) = 0, \quad \text{for } i = 1, 2, 3, 4. \tag{4.2}$$

Using the Newton–Raphson method, we solve equations (4.2), linearized with respect to $d\lambda, d\xi_2, d\xi_3$ and $d\xi_4$, to obtain an improved approximation, and this is done iteratively till convergence is obtained.

Before compressive loads are applied to the panel the solution is $(\lambda, \xi_1, \xi_2, \xi_3, \xi_4)$ $= (0, 0, 0, 0, 0)$. Starting with this solution, we use the Newton–Raphson method to plot λ against ξ_1 and thus determine the maximum value λ^* attained by the load parameter.
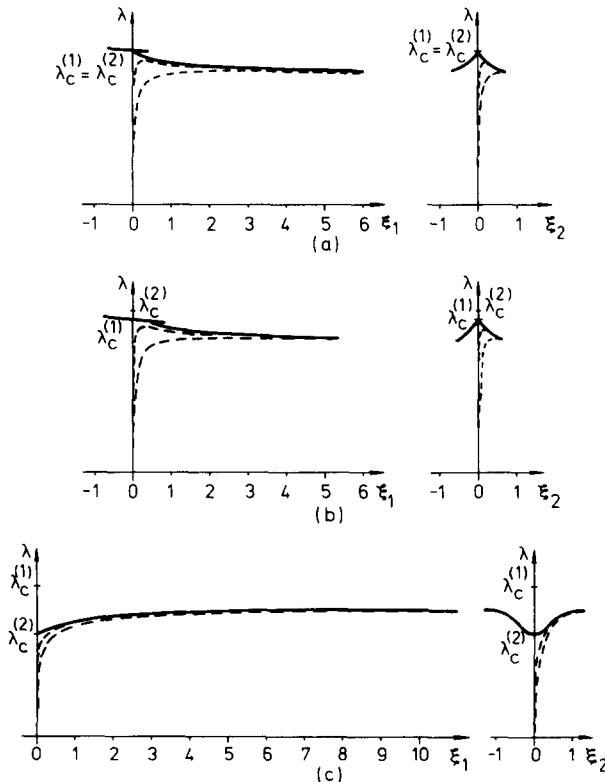
FIG. 2. Dependence on load of mode deflections. Solid curves correspond to perfect panels. Dashed curves correspond to imperfect panels.

When imperfections are present only in the shape of the Euler buckling mode ($\bar{\xi}_1 > 0$, $\bar{\xi}_2 = 0$), ξ_2 and ξ_4 remain equal to zero while ξ_1 and ξ_3 increase until the coefficient matrix of the linearized equations (4.2) becomes singular. At this point, bifurcation in the shape of the local buckling mode occurs. Depending on the panel parameters, this bifurcation can occur before, at, or after, the point at which λ^* is attained. When there are also imperfections in the shape of the local buckling mode ($\bar{\xi}_2 \neq 0$), the mode amplitudes ξ_1, ξ_2, ξ_3 and ξ_4 increase simultaneously with increasing λ until a limit point is reached.

Some examples of the relationship between load and mode deflections are shown in Fig. 2. The solid curves give the behaviour of a perfect panel, and the dashed curves show the behaviour of a panel with small initial imperfections. Only the dependence between λ, ξ_1 and ξ_2 has been shown, but the curves are based on a solution of equations (3.6).

The panel corresponding to Fig. 2a has coincident buckling loads, while Euler-type buckling is critical in Fig. 2b, and local buckling is critical in Fig. 2c. In all three cases the initial post-buckling behaviour predicted by the Galerkin method agrees with that calculated by application of Koiter's general theory. However, as the mode deflections increase, the equilibrium curves tend to flatten out. For example, in the simultaneous buckling case of Fig. 2a, this means that the sensitivity to very small imperfections is as strong as predicted by the asymptotic solution, but for imperfections so large that the limit point occurs under the flat part of the solid curve, a further increase of the imperfections results in practically no extra reduction of the limit load λ^*.

The average axial compression of the panel can be measured by the generalized displacement

$$\Delta = N_x^o \int_0^a \int_0^b u_{,x} \, dy \, dx + N_s^o \int_0^a [u_{,x} - ew_{,xx}]_{y=b/2} \, dx$$

$$= N_x^o \int_0^a \int_0^b \left(\frac{1}{Eh} \{ \lambda N_x^o + f_{,yy} - vf_{,xx} \} - \tfrac{1}{2} w_{,x}^2 - \bar{w}_{,x} w_{,x} \right) dy \, dx$$

$$+ N_s^o \int_0^a \left[\frac{1}{Eh} \{ \lambda N_x^o + f_{,yy} - vf_{,xx} \} - \tfrac{1}{2} w_{,x}^2 - \bar{w}_{,x} w_{,x} - ew_{,xx} \right]_{y=b/2} dx. \qquad (4.3)$$

The significance of Δ is that $\lambda\Delta$ represents the drop in potential energy of the external load. Substituting the expressions (3.2)–(3.4) for $\bar{w}$, w and f, respectively, in equation (4.3) and carrying out the integrations, we find that Δ is given as a polynomial in terms of λ, ξ_1, ξ_2, ξ_3, ξ_4, $\bar{\xi}_1$ and $\bar{\xi}_2$. Thus, Δ can be calculated directly as soon as the buckling equations (3.6) have been solved, and the stiffness $d\lambda/d\Delta$ can also be calculated. In the following we shall take the stiffness in the nondimensional form

$$S = \frac{d\lambda}{d\Delta} \bigg/ \left(\frac{d\lambda}{d\Delta} \right)_o \qquad (4.4)$$

where the denominator is the prebuckling stiffness of the perfect structure.

5. OPTIMUM DESIGNS

Defining an optimally designed panel involves many parameters, such as the plate thickness, the eccentricity of the stiffeners, the spacing between the stiffeners and the shape

of the stiffeners. However, we shall restrict the number of parameters involved, as we wish mainly to investigate whether a simultaneous buckling mode design has the highest carrying capacity. Thus, we prescribe the distance a between the simple supports, the spacing b between the stiffeners, the eccentricity e of the stiffeners and the common material to be used in the whole panel. Furthermore, the stiffeners, attached to one side of the plate, are assumed to have rectangular cross-sections.

Now for a panel built of a given amount of material per unit width, i.e. a panel with a given value of h_o, the maximum carrying capacity λ^* can be calculated as a function of the imperfection amplitudes $\bar{\xi}_1$ and $\bar{\xi}_2$ and the parameter h/h_o, specifying the ratio between the amount of material in the plate and that in the whole panel. In the following, λ_o denotes the critical load parameter in the case where the stiffeners disappear completely ($h/h_o = 1$).

As a first example we consider a panel specified by $a/b = 4$, $e/b = 0.05$ and $h_o/b = 0.0128$, which at simultaneous buckling coincides with the example chosen in [5]. In Fig. 3 the maximum carrying capacities have been plotted against h/h_o for different amounts of imperfections in a case in which $\bar{\xi}_1$ equals $\bar{\xi}_2$ (note that the imperfections are normalized against h_o, so that imperfections corresponding to different points on a curve with constant $\bar{\xi}$ are equal relative to a constant number, but not relative to the current plate thickness). The figure also shows the point N at which the initial post-buckling behaviour of the perfect structure changes from stable to unstable according to the Koiter theory, and we see that the λ^* curve corresponding to very small imperfections intersects the $\lambda_c^{(2)}$ curve just below this point. The behaviour with imperfections only in the shape of the local buckling mode ($\bar{\xi}_1 = 0$) is shown in Fig. 4, and the behaviour if only Euler-type imperfections are present ($\bar{\xi}_2 = 0$) is shown in Fig. 5.
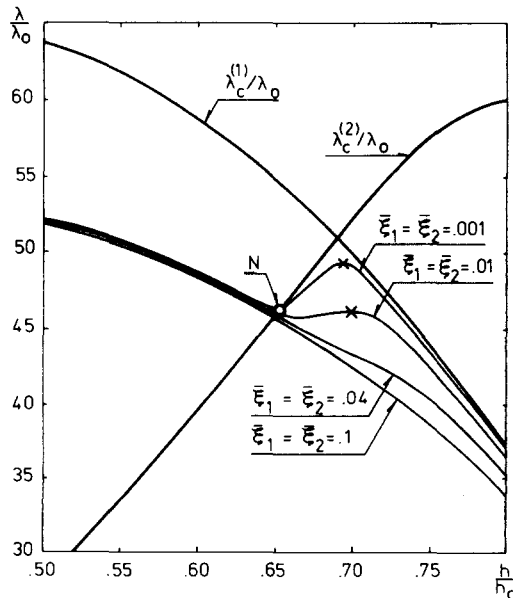
Fig. 3. Maximum carrying capacity λ^*/λ_o for a panel specified by $a/b = 0.4$, $e/b = 0.05$ and $h_o/b = 0.0128$ with imperfections $\bar{\xi}_1 = \bar{\xi}_2$.
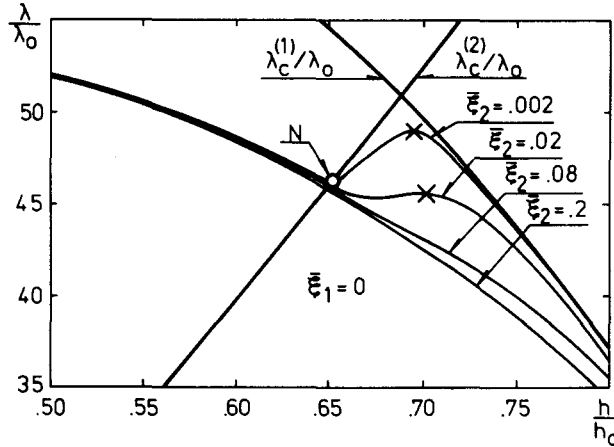
FIG. 4. Maximum carrying capacity λ^*/λ_o for a panel specified by $a/b = 4$, $e/b = 0.05$ and $h_o/b = 0.0128$ with only local mode imperfections.

If the panel is designed against the classical critical buckling stress, the optimum design is clearly the one with coincident buckling loads. However, Figs. 3–5 show that the carrying capacity in the vicinity of this design diminishes rapidly as small imperfections are introduced. The local maximum of the λ^* curves even vanishes when the imperfection amplitudes exceed a value of about 0.02 in Fig. 4 and about 0.08 in Fig. 5. The figures also show that the highest carrying capacities are predicted in the range where the local buckling stress $\lambda_c^{(2)}$ has been exceeded. Here, λ^* becomes even larger than the critical stress of the perfect structure in the simultaneous buckling case. In this range, however, the limit load λ^* corresponds to quite large mode deflections (Fig. 2c), so in practice plastic deformations may often reduce the maximum load predicted by the elastic theory.

Apart from a high limit load λ^*, the stiffness retained in the panel at a given load level may be of considerable interest too. For a perfect panel the stiffness S defined by equation (4.4) is equal to unity in the entire range below the classical buckling load. In Fig. 6 the
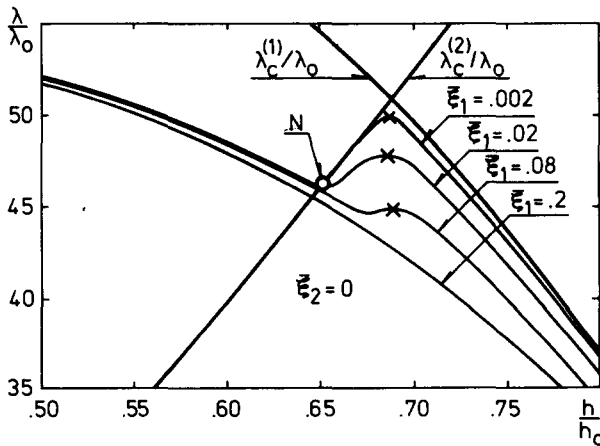
FIG. 5. Maximum carrying capacity λ^*/λ_o for a panel specified by $a/b = 4$, $e/b = 0.05$ and $h_o/b = 0.0128$ with only Euler-type imperfections.

stiffness S has been plotted for two different imperfection magnitudes. It is seen that even for small imperfections the stiffness decreases significantly at relatively low loads in the range where λ^* exceeds $\lambda_c^{(2)}$, so that this range is not advantageous from the point of view of stiffness. Also for larger imperfections a design with $\lambda_c^{(2)}/\lambda_c^{(1)}$ a little above unity is preferable with respect to keeping a high stiffness in the panel.
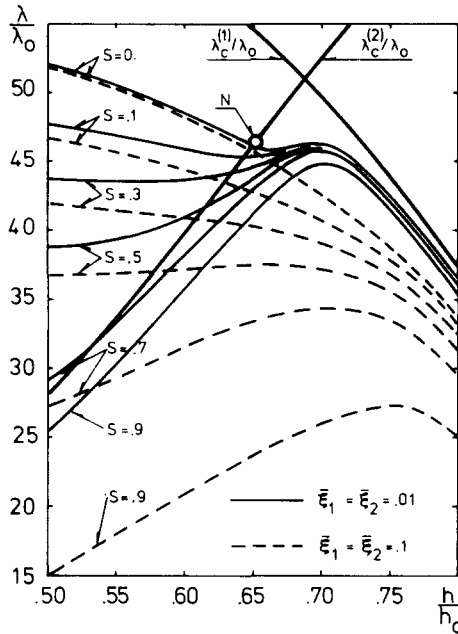
FIG. 6. Variation of the stiffness S with the load for two different imperfection magnitudes in a panel specified by $a/b = 4$, $e/b = 0.05$ and $h_o/b = 0.0128$.

As another example we shall try to halve the spacing between the stiffeners without changing the distance a between the supports, the eccentricity e of the stiffeners and the amount of material per unit width. In this case, the panel is specified by $a/b = 8$, $e/b = 0.1$ and $h_o/b = 0.0256$. For this panel the simultaneous buckling case corresponds to such a small value of h/h_o that further enlargement of the stiffeners at the expense of plate thickness is of practically no advantage with respect to $\lambda_c^{(1)}$, as can be seen in Fig. 7. Figures 7–9 show that the larger the relative amount of the local imperfections, the higher will be the value of h/h_o at which the maxima of the λ^* curves occur. It can also be seen that local mode imperfections of a given amplitude are more serious than Euler-type imperfections of the same amplitude. Finally, the variation of the stiffness S with the load is shown in Fig. 10 for two different magnitudes of imperfections.

In the present example, the carrying capacities predicted in the range where λ^* exceeds $\lambda_c^{(2)}$ are not larger than those in the remaining range, as they were in our first example. If imperfections can be kept small, the optimum design will correspond to values of $\lambda_c^{(2)}/\lambda_c^{(1)}$ slightly higher than unity, but for larger imperfections, this value increases to about two, depending on the stiffness required, if any, and on the imperfections.
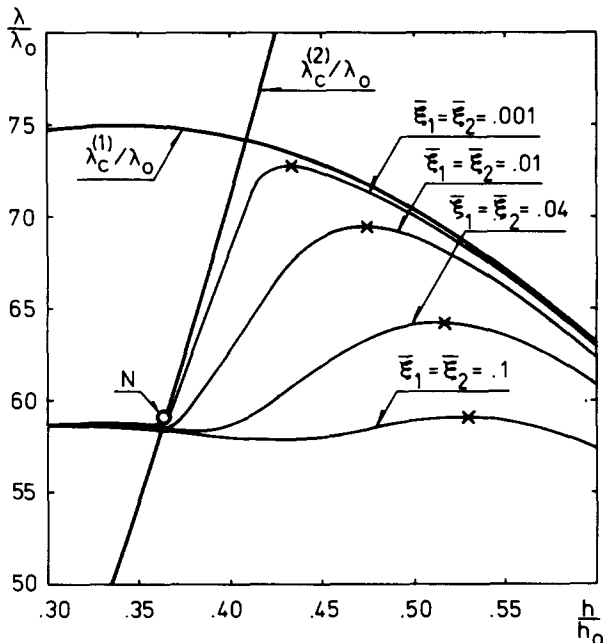
FIG. 7. Maximum carrying capacity λ^*/λ_o for a panel specified by $a/b = 8$, $e/b = 0.1$ and $h_o/b = 0.0256$ with imperfections $\bar{\xi}_1 = \bar{\xi}_2$.

CONCLUSION

An analysis of stiffened panels made of a given amount of material per unit width shows that in some cases the design with the highest carrying capacity is one in which the limit load is attained beyond the critical stress for local buckling. However, the stiffness properties are relatively poor for such designs. From the point of view of retaining a high
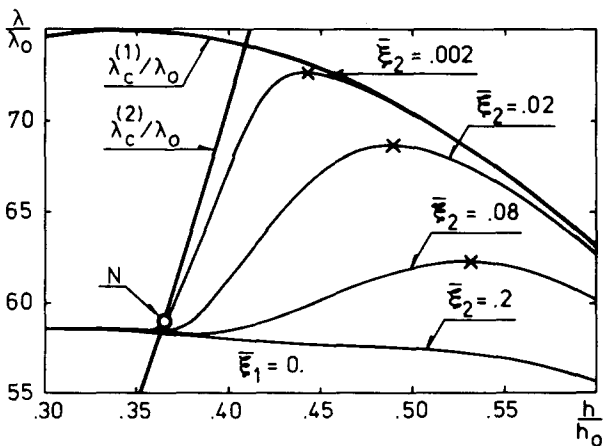
FIG. 8. Maximum carrying capacity λ^*/λ_o for a panel specified by $a/b = 8$, $e/b = 0.1$ and $h_o/b = 0.0256$ with only local mode imperfections.
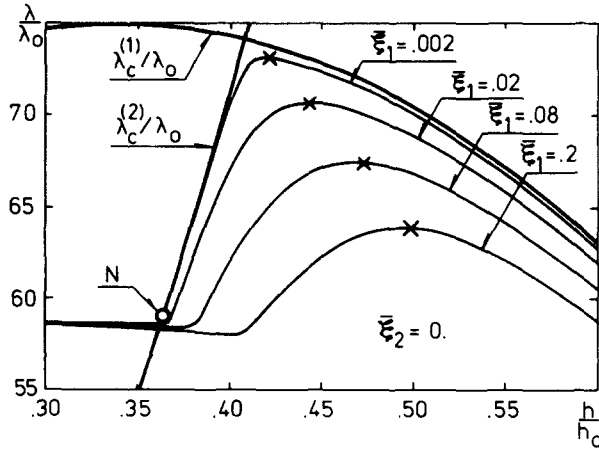
FIG. 9. Maximum carrying capacity λ^*/λ_0 for a panel specified by $a/b = 8$, $e/b = 0\cdot1$ and $h_o/b = 0\cdot0256$ with only Euler-type imperfections.

stiffness at the highest possible load level, the best design is usually one in which the critical stress for Euler-type buckling is smaller than that for local buckling. In some cases, the optimum design has a local buckling stress that is more than twice the Euler buckling stress. Thus, the optimum design from the point of view of post-buckling behaviour often differs significantly from the design with two simultaneous buckling stresses.
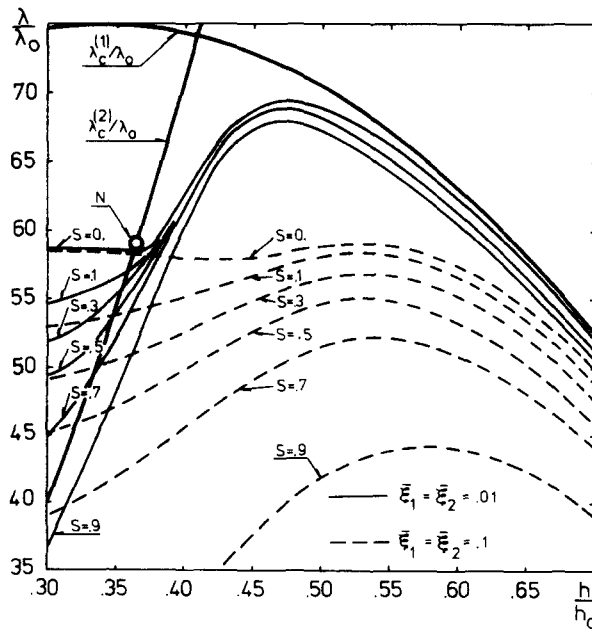
FIG. 10. Variation of the stiffness S with the load for two different imperfection magnitudes in a panel specified by $a/b = 8$, $e/b = 0\cdot1$ and $h_o/b = 0\cdot0256$.

REFERENCES

[1] F. CAMPUS and C. MASSONET, Colloque sur le comportement postcritique des plaques utilisées en construction métallique. Interventions de W. T. KOITER et M. SKALOUD, pp. 64–68; 103; 104. Mémoires de la Société Royale des Sciences de Liege, 5me série, tome VIII, fascicule 5 (1963).
[2] A. VAN DER NEUT, The interaction of local buckling and column failure of thin-walled compression members. *Proc. 12th Int. Congr. Appl. Mech.*, Stanford University 1968. Springer (1969).
[3] W. T. KOITER and G. D. C. KUIKEN, The interaction between local buckling and overall buckling on the behaviour of built-up columns. Delft lab. Report—WTHD 23, May (1971).
[4] J. M. T. THOMPSON and G. M. LEWIS, On the optimum design of thin-walled compression members. *J. Mech. Phys. Solids* **20**, 101–109 (1972).
[5] V. TVERGAARD, Imperfection-sensitivity of a wide integrally stiffened panel under compression. *Int. J. Solids Struct.* **9**, 177–192 (1973).
[6] W. T. KOITER, Over de stabiliteit van het elastisch evenwicht. Thesis, Delft, H. J. Paris, Amsterdam 1945. English translation issued as NASA TT F-10, 833 (1967).
[7] B. BUDIANSKY and J. W. HUTCHINSON, Dynamic buckling of imperfection-sensitive structures. *Proc. XI Int. Congr. Appl. Mech.*, Munich, pp. 636–651. Springer (1964).
[8] J. W. HUTCHINSON, Axial buckling of pressurized imperfect cylindrical shells. *AIAA J.* **3**, 1461–1466 (1965).

Абстракт—Для широкой панели, эксцентрично подкрепленной ребрами жесткости, нагруженной сжимаемой нагрузкой, исследуется расчет на минимум материала, при одновременном наличии продольного изгиба в смысле широкой колонны типа Эйлера и учета местного выпучивания пластинки между ребрами жесткости. Задано суммарное количество материала на единицу широты панели. Путем применения метола Галеркина, подсчитываются приблизительно максимальные несущие способности, в виде функции распределения этого материала в пластинке и ребрах жесткости. Опнределяются расчет для найлучшей несущей способности и для найлучшей способности, сохраняющей особую жесткость, в соответствии к заданным неточностям. Указано, что неточности удаляют оптимум от совпадающего расчета форм выпучивания.